

# Directed flow of $\Lambda$ , $\bar{\Lambda}$ , $K^\pm$ , $K_S^0$ and $\phi$ mesons from Beam Energy Scan Au+Au collisions using the STAR experiment

Subhash Singha (for the STAR collaboration)

*Department of Physics, Kent State University, Ohio 44242, USA*

E-mail: [subhash@rcf.rhic.bnl.gov](mailto:subhash@rcf.rhic.bnl.gov)

**Abstract.** We report the results of  $v_1$  and  $dv_1/dy$  near mid-rapidity for  $\Lambda$ ,  $\bar{\Lambda}$ ,  $K^\pm$ ,  $K_S^0$  and  $\phi$  in Au+Au collisions at  $\sqrt{s_{NN}} = 7.7, 11.5, 14.5, 19.6, 27$  and  $39$  GeV using the STAR detector at RHIC. The  $dv_1/dy$  of  $\Lambda$  is found to be consistent with that of the proton and shows a change in sign near  $\sqrt{s_{NN}} = 11.5$  GeV. The  $v_1$  slope for  $\bar{\Lambda}$ ,  $\bar{p}$  and  $\phi$  shows a similar trend for  $\sqrt{s_{NN}} > 14.5$  GeV, while below  $14.5$  GeV,  $\phi$   $v_1$  is consistent with zero but with a large uncertainty. The  $dv_1/dy$  for net protons and net kaons is similar for  $\sqrt{s_{NN}} > 14.5$  GeV, but they deviate at lower beam energies.

## 1. Introduction

The measurement of collective flow in relativistic heavy-ion collisions can offer an insight into the Equation of State (EoS) of the QCD matter produced in early stages of the collision [1]. The directed flow ( $v_1$ ) is characterized by the first harmonic coefficient in the Fourier expansion of the azimuthal distribution of the produced particles with respect to the reaction plane ( $\Psi_R$ ), i.e.,  $v_1 \equiv \langle \cos(\varphi - \Psi_R) \rangle$ , where  $\varphi$  denotes the azimuthal angle of the produced particles [2]. Both hydrodynamic [3, 4] and transport model [5] calculations imply that  $v_1$  is sensitive to the EoS and is a promising observable to explore the QCD phase diagram. One of the main goals of the Beam Energy Scan (BES) program at RHIC is to search for signatures of a possible QCD critical point and first-order phase transition [6, 7, 8]. Recently, STAR published the beam energy dependence of the slope of directed flow ( $dv_1/dy$ ) for protons and net protons near mid-rapidity [9]. The observation of a minimum in the slope of directed flow for protons and net protons around  $\sqrt{s_{NN}} = 10$ - $20$  GeV, and a double sign change in this observable for net protons, point to a possible softening of the QCD equation of state [10]. However, other recent model calculations, with and without crossover and first-order phase transitions, show large discrepancies with the STAR measurements [10, 11, 12, 13].

A new set of measurements with different hadron species ( $\Lambda$ ,  $\bar{\Lambda}$ ,  $K^\pm$ ,  $K_S^0$  and  $\phi$ ), and hence different constituent quarks, will not only help to understand the QCD phase transition, but in addition will allow to disentangle the role of produced and transported quarks in heavy-ion collisions. In particular, the  $\phi$  meson offers a unique advantage because its mass is similar to the proton mass, yet it is a vector meson. Moreover  $\phi$  meson is minimally affected by late-stage hadronic interactions.

## 2. Analysis Details

The  $v_1$  analysis is applied to data taken by the STAR detector during 2010, 2011 and 2014. The STAR detector offers uniform acceptance, full azimuthal coverage, and excellent particle identification. The Time Projection Chamber (TPC) [14] performed charged particle tracking near mid-rapidity. The collision centrality is estimated from the charged particle multiplicity within the pseudorapidity region  $|\eta| < 0.5$ . Particles are identified using both the Time Projection Chamber (TPC) and Time of Flight (TOF) [15] detectors. Two Beam Beam Counters (BBC) [16], covering  $3.3 < |\eta| < 5.2$ , are used to reconstruct the event plane. The BBC event plane is based on the first harmonic, since the  $v_1$  signal is strong in the BBC acceptance region at BES energies. Moreover, a large  $\eta$ -gap relative to the TPC reduces non-flow effects [2] in the  $v_1$  measurements. The uncharged particle species are measured through the reconstruction of the topology of their weak decays into charged particles:  $K_s^0 \rightarrow \pi^+\pi^-$ ,  $\Lambda \rightarrow p\pi$  (and charge conjugates for anti-particles). Topological selection cuts are applied in order to reduce backgrounds without much loss of the signal. The  $\phi$  meson is measured using its hadronic decay channel:  $\phi \rightarrow K^+K^-$ . The  $v_1$  for these particles is extracted by an invariant mass method [17].

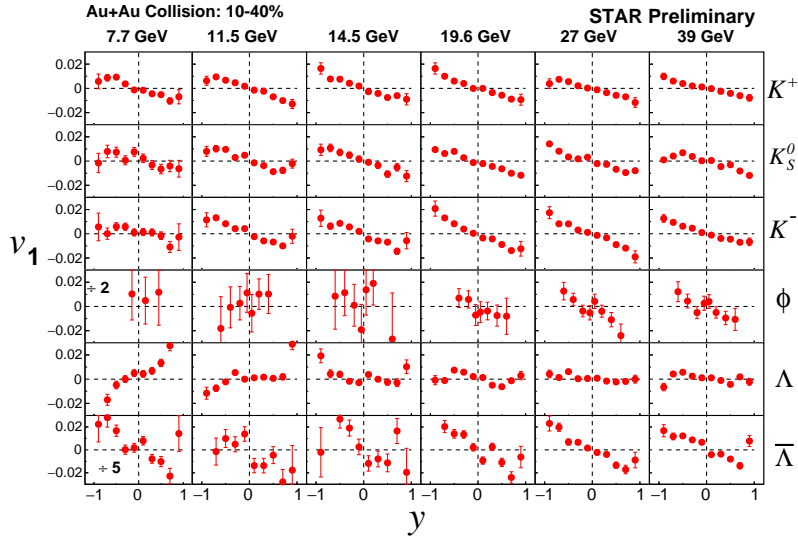


**Figure 1.** Rapidity dependence of  $v_1$  for  $K^\pm$ ,  $K_s^0$ ,  $\phi$ ,  $\Lambda$  and  $\bar{\Lambda}$  in 10-40% Au+Au collisions at  $\sqrt{s_{\text{NN}}} = 7.7, 11.5, 14.5, 19.6, 27$  and  $39$  GeV.

## 3. Results and Discussion

Figure 1 presents  $v_1$  as a function of rapidity for  $K^\pm$ ,  $K_s^0$ ,  $\phi$ ,  $\Lambda$  and  $\bar{\Lambda}$  in 10-40% Au+Au collisions at  $\sqrt{s_{\text{NN}}} = 7.7, 11.5, 14.5, 19.6, 27$  and  $39$  GeV. The data points for  $\bar{\Lambda}$  and  $\phi$  at  $7.7$  GeV are divided by factors of  $5$  and  $2$ , respectively, in order to use the same vertical scale in all panels. In a previous analysis, the  $v_1(y)$  slope parameter near mid-rapidity was extracted by fitting it with a cubic function [9]. Although the cubic fit reduces sensitivity to the rapidity range where the fit is performed, it is unstable for particles with poor statistics (e.g.  $\phi$  and  $\bar{\Lambda}$ ). Therefore in Ref. [18] and the present analysis, the  $v_1$  slope is based on a linear fit within the range  $|y| < 0.8$  for all particle species and all energies. All kaons and  $\bar{\Lambda}$  show a negative slope at all beam energies. The  $\phi$  meson shows a negative slope at  $\sqrt{s_{\text{NN}}} > 14.5$  GeV. The  $dv_1/dy$  for all the measured strange hadrons is shown in Fig. 2. The  $dv_1/dy$  of  $\Lambda$  is consistent with

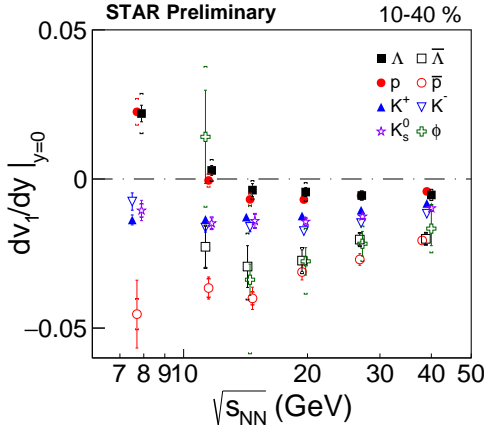


**Figure 2.** (Color online) Beam energy dependence of  $dv_1/dy$  for  $p$ ,  $\bar{p}$ ,  $K^\pm$ ,  $K_s^0$ ,  $\phi$ ,  $\Lambda$  and  $\bar{\Lambda}$  in 10-40% Au+Au collisions.

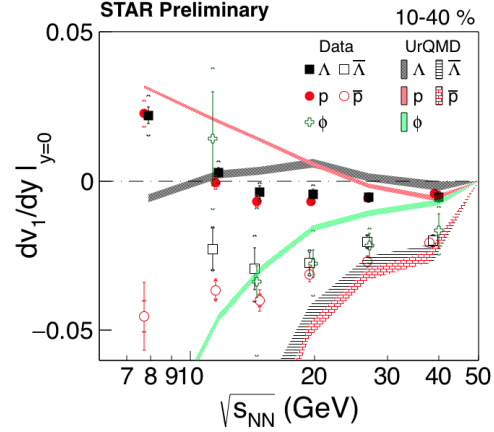


**Figure 3.** (Color online) Beam energy dependence of  $dv_1/dy$  for  $p$ ,  $\bar{p}$ ,  $\phi$ ,  $\Lambda$  and  $\bar{\Lambda}$  in 10-40% Au+Au collisions. STAR data are compared with UrQMD [5] model calculations.

that of protons at all beam energies, while the  $\bar{\Lambda}$  follows the trend of antiprotons. The  $dv_1/dy$  for  $K^+$  is closer to zero than that for  $K^-$  for  $\sqrt{s_{NN}} > 11.5$  GeV, while the trend is reversed at 7.7 GeV. The  $K_s^0$   $dv_1/dy$  lies between  $K^+$  and  $K^-$  at all beam energies. Theorists [19] have argued that kaon-nucleon potentials influence directed flow at these energies, where the baryon density is high. The  $dv_1/dy$  for  $\phi$  shows similar trends as  $\bar{\Lambda}$  and  $\bar{p}$  for  $\sqrt{s_{NN}} > 14.5$  GeV, while at 11.5 GeV,  $dv_1/dy$  for  $\phi$  is consistent with zero with large uncertainty. In the higher energy region where antibaryon production is significant,  $\bar{p}$ ,  $\phi$  and  $\bar{\Lambda}$  show similar energy dependence. Figure 3 presents a comparison between the measurements and UrQMD [5] for  $p$ ,  $\Lambda$  and  $\phi$ . UrQMD seems to follow the trend of the data for higher beam energies, but deviates at lower energies. Figure 4 shows the  $dv_1/dy$  of  $p$ ,  $K^+$ ,  $\pi^-$  and  $K_s^0$  on the left panel, and corresponding anti-particles in the right panel, as a function of beam energy. Here the particles in the left panel are expected to have more quarks from stopped initial-state nucleons than the antiparticles on the right. The charged kaons and  $K_s^0$  are compared with UrQMD [5] and HSD [13] model calculations. Both models qualitatively describe the data at higher energies, but fail to follow the trend of the data at lower energies. Figure 5 shows a comparison of the beam energy dependence of  $dv_1/dy$  for net protons and net kaons. Study of net particle  $v_1$  is motivated by the goal of separating the contributions from produced quarks versus quarks that are transported from the initial state. We define

$$F_p = r_1(y)F_{\bar{p}} + (1 + r_1(y))F_{\text{net-}p} \quad (1)$$

$$F_{K^+} = r_2(y)F_{K^-} + (1 + r_2(y))F_{\text{net-}K} \quad (2)$$

where  $F$  denotes  $dv_1/dy$  for the indicated particle species;  $r_1(y)$  and  $r_2(y)$  are the rapidity dependence of the ratios of the corresponding antiparticles to particles. It is observed that net- $p$  and net- $K$   $dv_1/dy$  follow a similar trend for  $\sqrt{s_{NN}} = 14.5 - 200$  GeV, while they deviate from each other strongly at 7.7 GeV.

#### 4. Summary

In these proceedings, we present  $v_1$  and  $dv_1/dy$  measurements of strange hadrons from the STAR experiment at RHIC. The  $\Lambda$   $dv_1/dy$  is consistent with the proton  $dv_1/dy$  and both show a sign change near  $\sqrt{s_{NN}} = 11.5$  GeV. Charged kaons and  $K_s^0$  show negative  $v_1$  for all studied beam

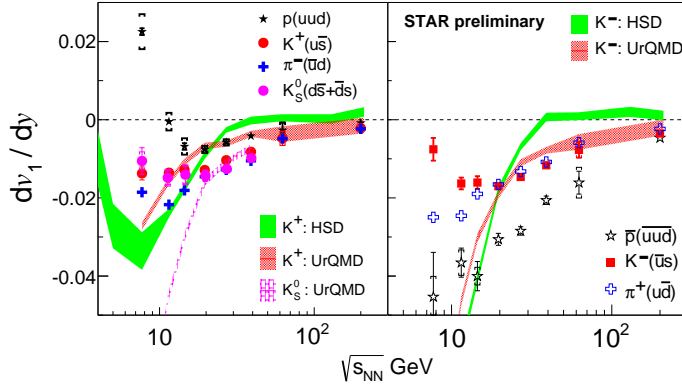


**Figure 4.** (Color online) Left Panel: Beam energy dependence of  $dv_1/dy$  for  $p$ ,  $K^+$ ,  $\pi^-$  and  $K_s^0$  in 10-40% Au+Au collisions. Right panel: Beam energy dependence of  $dv_1/dy$  for  $\bar{p}$ ,  $K^-$ ,  $\pi^+$  in 10-40% Au+Au collisions. HSD [13] and UrQMD [5] model calculations are shown for  $K^\pm$  and  $K_s^0$ .

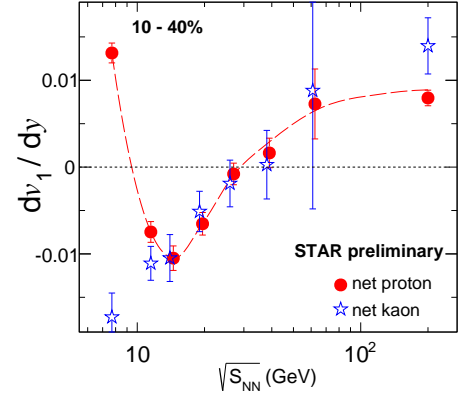


**Figure 5.** (Color online) Beam Energy dependence of net-particle  $dv_1/dy$  in 10-40% Au+Au collisions.

energies, while the  $K_s^0$  lies between the charged kaons.  $\bar{\Lambda}$ ,  $\bar{p}$  and  $\phi$  show similar  $v_1$  slope for  $\sqrt{s_{NN}} > 11.5$  GeV. The UrQMD and HSD results qualitatively explain the data at higher beam energies, but fail to describe the trend observed at lower energies.

## References

- [1] W. Reisdorf and H. G. Ritter, Annu. Rev. Nucl. Part. Sci. **47**, 663 (1997); H. Sorge, Phys. Rev. Lett. **78**, 2309 (1997).
- [2] A. M. Poskanzer and S. A. Voloshin, Phys. Rev. C **58**, 1671 (1998); S. Voloshin and Y. Zhang, Z. Phys. C **70**, 665 (1996).
- [3] U. W. Heinz, in *Relativistic Heavy Ion Physics*, Landolt-Boernstein New Series, Vol. I/23, edited by R. Stock (Springer Verlag, New York, 2010).
- [4] H. Stöcker, Nucl. Phys. **A750**, 121 (2005).
- [5] S. A. Bass et al., Prog. Part. Nucl. Phys. **41**, 255 (1998); M. Bleicher, E. Zabrodin, C. Spieles, S. A. Bass, C. Ernst, S. Soff, L. Bravina, M. Belkacem, H. Weber, H. Stöcker and W. Greiner, J. Phys. G **25**, 1859 (1999).
- [6] B. I. Abelev *et al.* (STAR collaboration), STAR Note SN0493 (2009).
- [7] M. M. Aggarwal *et al.* (STAR collaboration), arXiv:1007.2613.
- [8] STAR collaboration, BES Phase-II Whitepaper, STAR Note SN0598 (2014).
- [9] L. Adamczyk *et al.* (STAR Collaboration), Phys. Rev. Lett. **112**, 162301 (2014).
- [10] Y. Nara, H. Niemi, A. Ohnishi, and H. Stöcker, arXiv:1601.07692 [hep-ph].
- [11] J. Steinheimer, J. Auvinen, H. Petersen, M. Bleicher and H. Stöcker, Phys. Rev. C **89**, 054913 (2014).
- [12] Yu. B. Ivanov, V. N. Russkikh, and V. D. Toneev, Phys. Rev. C **73**, 044904 (2006).
- [13] V. P. Konchakovski, W. Cassing, Yu. B. Ivanov and V. D. Toneev, Phys. Rev. C **90**, 014903 (2014).
- [14] M. Anderson *et al.*, Nucl. Instr. Meth. A **499**, (2003) 659.
- [15] W.J. Llope (STAR Collaboration), Nucl. Inst. and Methods A **661**, (2012) S110
- [16] C. A. Whitten (STAR Collaboration), AIP Conf. Proc. **980**, (2008) 390.
- [17] N. Borghini and J. Y. Ollitrault, Phys. Rev. C **70**, 064905 (2004).
- [18] P. Shanmuganathan for the STAR Collaboration, Proc. of Quark Matter 2015, Kobe, Japan, Nucl. Phys. **A** (in press); arXiv:1512.09009v1.
- [19] W. Cassing, V. P. Konchakovski, A. Palmese, V. D. Toneev, E. L. Bratkovskaya, EPJ Web Conf. **95**, 01004 (2015), arXiv:1408.4313, and references therein.